Low Temperature Physics/Fizika Nizkikh Temperatur, 2021, vol. 47, No. 3, pp. 227–234

Composite films of graphene oxide with semiconducting carbon nanotubes: Raman spectroscopy characterization

N. V. Kurnosov and V. A. Karachevtsev

B. Verkin Institute for Low Temperature Physics and Engineering of the National Academy of Sciences of Ukraine
Kharkiv 61103, Ukraine
E-mail: n.kurnosov@ilt.kharkov.ua

Received October 16, 2020, published online January 26, 2021

Noncovalent interaction between semiconducting single-walled carbon nanotubes (SWNTs) and graphene oxide (GO) in composite films (GO-SWNTs) was analyzed by Raman spectroscopy in the range of *D* and *G* modes (1170–1780 cm^{-1}). Comparison between Raman spectra of composite film and single-component GO and SWNTs films showed that the interaction between GO and SWNTs is accompanied by a band broadening and spectral shifting. Observed spectral transformations are attributed to charge transfer between GO and SWNTs as well as a deformation of carbon surfaces which occurs in the composite. Spectral measurements of composite GO-SWNTs film with biological globular molecules (the enzyme glucoseoxidase) showed that these molecules weaken mechanical stress of GO on the nanotubes.

Keywords: graphene oxide, single-walled carbon nanotubes, composite films, noncovalent interaction, Raman spectroscopy.

1. Introduction

Analysis of investigations of graphene nanomaterials performed lately has shown that graphene derivatives are of essential interest among researchers which is even more persistent than that to pristine graphene. Among these derivatives graphene oxide (GO) has attracted the most attention [1–4]. GO is an oxygenated graphene sheet. Graphene oxide can be prepared in large scale through the chemical exfoliation method from graphite that makes it the very low-cost graphene derivative. Oxygen-containing groups bound to graphene facilitate its following chemical functionalization with different organic and biological molecules that essentially extends the area of practical applications of GO [5]. However, GO has an essential drawback, this graphene derivative is an electrically insulating material. Electrical properties of GO can be improved through chemical/thermal reduction processes or by the preparation of composites with conductive nanomaterials. In latter case, the carbon nanotubes are ideal component for the fabrication of the conductive composite with GO. Notably, the single-walled carbon nanotubes are especially perspective, as bulk synthesis produces a set of different metallic and semiconductor nanotube species (conductivity is explicitly determined by nanotube chirality). The different ratio of metallic/semiconducting conductivities in a sample also influences on the properties of prepared composites with GO. A few methods are used to prepare such composites including a layer-by-layer deposition, deposition from suspension under pressure (spray method), vacuum filtration, and chemical vapor deposition. In composite SWNTs are randomly distributed between GO sheets preventing them from re-sticking together forming films like a paper. At certain GO:SWNTs ratio the nanotubes will provide a conductivity of such composite film.

Electrical conductivity in individual SWNTs, bundles, nanotube networks, and thin and bulk films has been studied by a few groups (see in Refs. 6–10). It occurred that the conductivity of nanotube networks and films depends on the type of conductivity in individual nanotubes, their length and diameter, the ratio of metallic nanotubes to semiconducting ones, film thickness, extent of doping, etc. Note that the most complete information about a specific electron transport mechanism in such systems is mainly extracted from the analysis of the temperature dependence of the electrical conductivity. It was shown that the motion of electrons in nanotube networks or films depends on potential barriers between the nanotubes at their contacts. The role of these contacts is especially manifested at low temperatures. The main mechanism that explains the conductivity in carbon nanotube systems at low temperatures is the tunneling of thermally activated electrons through barriers [6–11] while at higher temperatures the conductivity depends on the electron hopping over barriers. As our investigations

have shown, these mechanisms may describe the temperature dependence of the electrical conductivity of composite GO-SWNTs films too [12, 13]. Measurement of electrical transport demonstrated that GO-SWNTs and SWNTs films exhibit a decrease in electrical conductivity with decreasing temperature that indicates similarity with the electrical conductivity in disordered semiconductor systems [14]. From the analysis of the temperature dependence of the electrical conductivity, the parameters of the electron transport in the GO-SWNTs and the SWNTs films were estimated: the average electron hopping length (r) and hopping energy (W), plotted their temperature dependences, and determined the potential barrier height (E_G) [12]. It was revealed that the resistivity of the GO-SWNTs composite film is larger than for the SWNTs film in the wide temperature range (from 5 to 291 K), as well as evaluated W parameter. The potential barrier value the E_G obtained by approximation of resistance temperature dependence $R(T)$ with the Arrhenius formula in a temperature range of 240–291 K is also larger for the composite film (18 vs 11 meV). The analysis of transport parameters performed for the different films showed that nanotube contact with the GO surface hinders an electron transport in the composite film.

In addition to obtaining a number of parameters of the electron transport in composite GO-SWNTs films, it is necessary to clarify the details of the interaction between GO surface and SWNT needed for a wider use of the composites in applications. The key questions in this analysis concern the charge transfer between GO and SWNT and the structural deformations in each components of the nanohybrid appearing as a result of the interaction. Such method as Raman spectroscopy can help to answer these questions. Raman features of both GO and SWNTs not only provide information concerning vibrational properties, but are also substantially governed by electron-phonon coupling thus causing changes in electronic structure to be manifested in Raman spectra. GO and SWNT mostly derive their vibrational properties from the Brillouin zone of graphene as a fundamental sp^2-bound carbon structure [15, 16]. Graphene in-plane optical phonon branches give rise to the G band which is observed in Raman spectra of GO and SWNTs. There are certain structure-related peculiarities of this band needed to be mentioned. The curvature of SWNT surface causes splitting of G band into so-called G^+ and G^- bands, which are attributed to vibrations along the nanotube axis and in circumferential directions, respectively. In addition, the G^- band of metallic SWNT is often asymmetric due to specific electron-phonon coupling and displays Breit–Wigner–Fano lineshape [17]. The G band of graphene oxide is much broader as compared to graphene (~ 100 and ~ 10 cm^{-1}, respectively). This is in analogy to broadening that takes place when initially regular monolayer graphene becomes more disordered and inhomogeneous because of randomly introduced defects [18]. In case of graphene oxide, the bound oxygen groups of different types (carboxyl, carbonyl, epoxy, hydroxyl) serve as such defects. Moreover, they can be grouped together [19] and sp^2 and sp^3 bound domains are formed in GO, which affects the linewidth of Raman bands. The presence of defects also activates additional modes in the Raman spectrum of graphene-related materials. D mode is observed in both GO and SWNT spectra and is a one-phonon (tangential) one-elastic intervalley scattering process, while intravalley D' mode is present in defective graphene and GO [15–17]. It was shown that analysis of defect-induced modes relative intensity can be used for study of different defect types [20–22].

We had already performed the study of noncovalent coupling of SWNTs with GO employing optical spectroscopy, scanning microscopy, and theoretical calculations (molecular dynamics simulation and DFT calculation) [23]. In those experiments, we had used SWNTs grown by HiPCO method that produces metallic and semiconducting nanotubes in ratio of about 1:1. We had found the suppression of intensity of absorption bands related to the electronic transitions of semiconducting SWNTs that was explained by the charge transfer from these SWNTs to GO. The analysis of Raman spectra of the SWNT-GO film revealed the combined effect caused by the charge transfer between components and the strong coupling that induced the stress and the structural deformations in the carbon nanostructures. This observation was confirmed by DFT calculations that show the deformation of the SWNTs and the GO in the nanohybrids.

In this work, we extend our analysis of the GO-SWNTs films employing Raman spectroscopy and select nanotube samples that contain predominantly semiconducting nanotubes (~ 95 %). To verify a stress factor we have also prepared composite GO-SWNTs film with an addition of biological globules [enzyme glucose oxidase (GOx)]. The diameter of this globule is more than 4 nm that exceeds diameters of individual nanotubes (~ 0.8–1 nm) or their small bundles. It was supposed that globules located among GO sheets will weaken a mechanical stress of GO on the nanotubes.

2. Experimental details

2.1. Materials

Graphene oxide used in experiments was purchased from Graphenea (San Sebastian, Spain). GO was synthesized by modified Hummers' method [24]; the content of C and O in raw material is designated as 49–56 % and 41–50 %, respectively (C:O ratio is equal 1.2:1.3). The SWNTs grown by CoMoCAT method were purchased from SouthWest NanoTechnologies (USA). According to the manufacturer's data, the content of metallic SWNTs is less than 5 %, so the semiconducting species are prevalent and (6,5) chirality constitutes more than 50 % of all synthesized SWNTs. Glucose oxidase (GOx) from Aspergillus niger was purchased from Sigma–Aldrich (USA).

2.2. Preparation of single-component GO, SWNTs and composite GO-SWNTs, GO-SWNTs-GOx films

Nanotubes were ultrasonicated in acetone solution for 40 min, the obtained stable suspension (SWNTs concentration 0.2 mg/ml) was deposited onto PTFE membrane (diameter 12.5 mm, pores 0.24 μm, Millipore, USA) by vacuum filtration. The resulting film surface density was 0.3–0.4 mg/cm^2, the thickness ~ 10 μm. The GO film was obtained similarly from GO aqueous suspension (0.2 mg/ml) that contained mainly monolayers [5]. For preparation of the composite, the nanotubes were added to the GO aqueous suspension and sonicated for 40 min. The composite GO-SWNTs film was also formed by vacuum filtration of respective aqueous suspension. It was found that the film is flexible, porous, and water-permeable [14]. The mass ratio of graphene oxide and nanotubes in suspension was 1:1. The glucose oxidase was added into already sonicated mixture of GO and SWNTs (0.05 mg/ml GOx concentration, GO:SWNTs:GOx ratio 4:4:1) in case of GO-SWNTs-GOx film preparation.

Additionally, the film containing SWNTs with adsorbed single-stranded DNA was used in experiments for comparative analysis. This film was obtained from SWNTs:DNA aqueous suspension (prepared by sonication for 60 min and 70000 g centrifugation) which was deposited on quartz substrate using the spray method.

2.3. Raman measurements

He–Ne laser (632.8 nm, 20 mW) was used for excitation of Raman scattering. Laser beam was focused on the surface of films into ~ 0.3 mm diameter spot to decrease heating and avoid sample damage. Spectra were analyzed using double grating monochromator and detected with electrically cooled CC*D* camera. Spectral slit width was 1.6–2 cm^{-1}. Plasma lines from He–Ne laser were used for an internal spectral calibration.

3. Results and discussion

An analysis of the noncovalent interaction between carbon nanotubes and GO in hybrids employing Raman spectroscopy is based on a comparison of Raman spectra of composite films with spectra of components. Thus we have studied the films which contain components present in composites (SWNTs and GO films) beforehand.

3.1. Raman spectroscopy of SWNTs and GO films

The Raman scattering spectrum of nanotube (SWNTs) film obtained by vacuum filtration is shown in Fig. 1(a).

Spectral features observed in 1170–1780 cm^{-1} range were attributed to SWNT Raman tangential and defect-induced modes [15, 17]. The experimental spectrum was fitted with a sum of Lorentzian functions. The broad band peaked at 1307 cm^{-1} was approximated well by a single Lorentzian. This band corresponds to defect *D* mode, which includes a non-zero wave vector phonons "activated" in Raman spectrum by elastic scattering on defects of the structure [15, 17]. The most intense sharp band with maximum at ~ 1593 cm^{-1} is caused by tangential vibrations along the nanotube axis and is denoted as G^+ band in literature. The less intense band located at lower-frequency slope of G^+ band is denoted as G^- band (it corresponds to circumferential tangential vibrations). The spectral range 1500–1650 cm^{-1} was fitted by 5 Lorentzian functions. The spectral parameters of all bands obtained at fitting of SWNTs spectrum are presented in Table 1. The resulting frequencies of tangential bands are 1519, 1541, 1551.8, 1592, and 1599.6 cm^{-1}. Three Lorentzians correspond to G^- band, other two are assigned to G^+ band and are used for precise approximation of this intense band. As the frequency difference between the G^+ and G^- modes depends on SWNT chirality indexes and diameter d_t [25, 26] (roughly proportional to $1/d_t^2$), the structured G^- mode can be explained by different

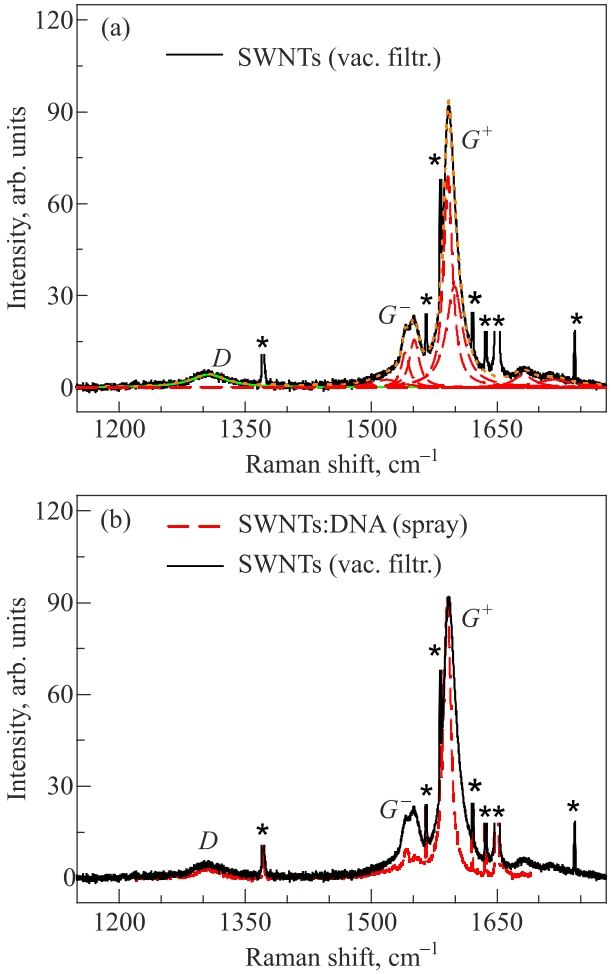

Fig. 1. (Color online) (a) Raman spectrum of the nanotube film. Solid lines under the experimental spectrum show its deconvolution obtained as a result of fitting to the sum of Lorentzians. Dashed line matching with the experimental spectrum represents the sum of all spectral functions. Asterisks * denote the He–Ne plasma lines. (b) Comparison between Raman spectra of nanotube film and of film containing SWNTs:DNA hybrids normalized to the G^+ band intensity.

Table 1. Frequency of maximum, full width at half maximum (FWHM) and integral intensity of Lorentzians obtained at the fitting of experimental Raman spectrum of SWNTs film

Mode	Frequency ω, cm^{-1}	FWHM Δ, cm^{-1}	Area, arb. units
D	1307.0	50.7	335
G^-	1519.0	40.0	156
G^-	1541.0	11.4	205
G^-	1551.8	13.6	334
G^+	1592.0	12.7	1378
G^+	1599.6	23.3	1208

SWNT species present in the film. We should also note that the Lorentzian component of G^+ band with maximum at ~ 1600 cm^{-1} present in SWNTs film spectrum was not observed in our experiments with isolated SWNTs in SWNTs:DNA hybrids [see Fig. 1(a), (b)]. We attribute this feature, which also causes an overall broader G^+ band in the case of SWNTs film, to nanotube bundles which can be formed at vacuum filtration process. This was further confirmed by analysis of G^- and G^+ band areas, as the presence of nanotube bundles increases the G^-/G^+ ratio [27]. Such ratio calculated using the sum of respective Lorentzian areas is 0.27 for SWNTs film (see Table 1) which is larger than 0.2 value obtained for our SWNTs:DNA sample. Note that according to analysis of G^- band and absence of asymmetrical Breit–Wigner–Fano components observed in the spectrum of HiPCO SWNTs [27], all nanotube bands manifested in the spectrum are assigned to semiconducting species [28].

The Raman spectrum of the GO film shown in Fig. 2 was registered in the same spectral range as that used for the SWNTs film.

The higher-frequency band at ~ 1600 cm^{-1} originates from the only first-order Raman-allowed band of graphene (G band) and corresponds to in-plane vibrations of sp^2-bonded carbon atoms. The band with maximum at ~ 1340 cm^{-1} was attributed to defect-induced (D) mode. This mode arises due to defects in graphene lattice [15–17] and therefore D mode is more manifested in GO samples as compared to single-layer graphene. The observed GO bands are much broader than SWNT features. One of the reasons behind the large spectral width of both D and G bands lies in the structural peculiarities of GO samples (distribution of GO flakes sizes and amount of bound oxygen groups). We have also performed the fitting of the GO experimental spectrum with a sum of Lorentzians. The spectral parameters obtained are presented in Table 2.

The lower-frequency band in the experimental GO spectrum was effectively approximated with one Lorentzian (position of maximum is 1335 cm^{-1}). However, it was found at our fitting procedure that the higher-frequency band has such lineshape that it can not be precisely approximated with a single spectral function (we have tested symmetric Lorentzian or Gaussian and asymmetric Breit–Wigner–Fano

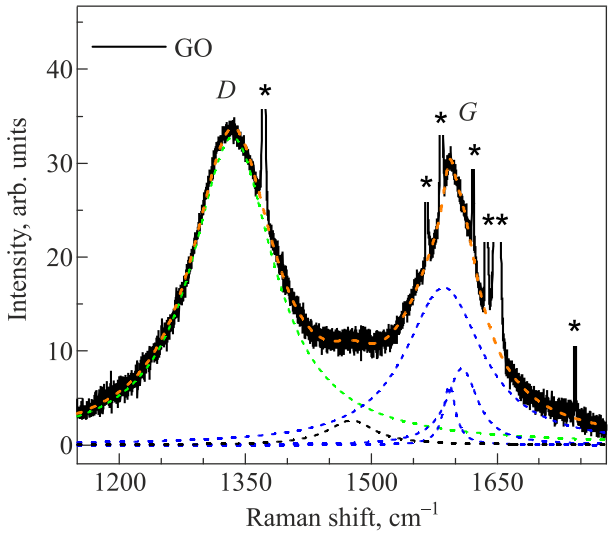

Fig. 2. (Color online) Raman spectrum of the GO film. Dashed lines under the experimental spectrum show its deconvolution obtained as a result of fitting to the sum of Lorentzians. Dashed line matching with the experimental spectrum represents the sum of spectral functions. Asterisks * denote the He–Ne plasma lines.

function). Eventually, apart from the wide and intense Lorentzian (position of maximum 1586 cm^{-1}), two narrow ones were included in the set of fitting spectral functions. Lorentzian peaked at 1608 cm^{-1} most probably corresponds to graphene intravalley defect-induced D' band [15–17] which is also observed in GO spectra [20, 21]. The position of maximum of the other narrow band (at 1593 cm^{-1}) almost perfectly matches with the more intense G^+ Lorentzian observed in the SWNTs spectrum. It is possible that this narrow and weak band ($G1$ in Table 2) can appear within the GO tangential mode range as a consequence of a curvature or bending of GO flakes. It is known that GO local bending occurs due to bound oxygen groups. The important role of oxidation degree in this regard was further confirmed in our Raman experiments with reduced GO films, which definitely contain smaller amount of bound oxygen groups. Reduced GO spectrum displayed none such narrow features within tangential bands. We should mention that at fitting of the GO spectrum we had to include into the approximation a rather weak band located between intense D and G bands as it was used in Refs. 21–23, 29. This in-

Table 2. Position of maximum, full width at half maximum (FWHM) and integral intensity of Lorentzians obtained at the fitting of experimental Raman spectrum of GO film

Mode	Frequency ω, cm^{-1}	FWHM Δ, cm^{-1}	Area, arb. units
D	1335.0	118.3	6085
D^{**}	1476.0	69.3	284
G	1586.3	111.4	2933
$G1$	1593.1	17.3	174
D'	1608.1	44.6	571

termediate band is denoted D^{**} in Table 2. The origin of D^{**} band in GO samples is somewhat ambiguous, it can appear due to the presence of bound hydrogen and C–H vibrations or be caused by remaining amorphous carbon according to Refs. 21, 22, 29.

The analysis of parameters of GO Raman bands allows to partially study GO defect properties. Firstly, the relative integral intensity of *D* band in GO spectrum correlates with the percentage of sp^2-hybridized carbon atoms [21], in more detail, the *D*/*G* ratio increases as the sp^2 percentage decreases. We deduce sp^2 domain fraction to be ~ 40 % or less using found *D*/*G* ratio of ~ 2 and data from Ref. 21. In addition, the large FWHM value of *G* and *D* bands (more than 100 cm^{-1}) also means highly disordered GO. Secondly, the simultaneous analysis of the relative integral intensity of *D* and *D′* bands is applicable for characterization of prevailing defect type (vacancies, edges, or sp^3 defects) according to Refs. 20, 21. The *D*/*D′* and *D′*/*G* ratios of ~ 11 and ~ 0.2 respectively mean that GO defects are mostly sp^3 defects which is fully understandable due to a chemical composition of our GO samples (nearly equal content of C and O).

3.2. Raman spectroscopy of GO-SWNTs composite film

Next, we have obtained and analyzed the Raman spectrum of the composite film containing both nanotubes and graphene oxide (GO-SWNTs) shown in Fig. 3.

As it follows from Figs. 1 and 2, the defect-induced and tangential bands of GO and SWNTs are located in the

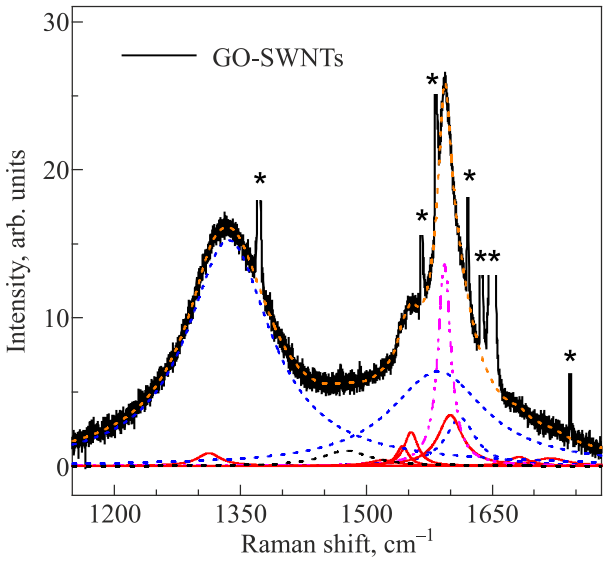

Fig. 3. (Color online) Raman spectrum of the composite film. Deconvolution into individual spectral functions is shown, dashed (blue and black) and solid (red) lines under the experimental spectrum represent bands originating from GO and SWNTs respectively; the dash-dotted line (crimson) is used for the band present in both SWNTs and GO films spectra (with maximum at 1593.1 cm^{-1}). Dashed line matching with the experimental spectrum represents the sum of all spectral functions. Asterisks * denote the He–Ne plasma lines.

Table 3. Position of maximum and full width at half maximum of spectral functions obtained at approximations of experimental spectra of single-component SWNTs, GO and composite GO-SWNTs and GO-SWNTs-GOx films. The normalized areas are put in brackets besides the frequency of corresponding band. Normalization in each case is to the area of the most intense tangential band

	Frequency ω, cm^{-1}				FWHM Δ, cm^{-1}			
Mode	GO	SWNTs	GO-SWNTs	GO-SWNTs-GOx	GO	SWNTs	GO-SWNTs	GO-SWNTs-GOx
D SWNTs		1307.0 (0.243)	1312.7 (0.032)	1308.2 (0.138)		50.7	33.5	42.6
D GO	1335.0 (2.07)		1336.1 (2.1)	1332.3 (2.21)	118.3		121.0	139.6
G^- SWNTs		1519.0 (0.11)	1520.0 (0.019)	1512.0 (0.044)		40.0	40.0	27.4
G^- SWNTs		1541.0 (0.148)	1543.2 (0.026)	1538.0 (0.045)		11.4	17	14.4
G^- SWNTs		1551.8 (0.24)	1553.4 (0.051)	1548.8 (0.081)		13.6	19.6	15.0
G GO (wide)	1586.3 (1)		1585.3 (1)	1586.5 (1)	111.4		137.8	113.8
G^+ SWNTs and/or G1 GO (narrow)	1593.1 (0.06)	1592.0 (1)	1593.1 (0.286)	1589.8 (0.396)	17.3	12.7	18.4	15.8
G^+ SWNTs		1599.6 (0.877)	1600.0 (0.137)	1598.1 (0.188)		23.3	35.0	20.2
D′ GO	1608.0 (0.19)		1612.0 (0.16)	1613.0 (0.217)	44.6		43.0	42.0

same spectral range. Thus an analysis of the Raman spectrum of GO-SWNTs composite is made complicated by overlapping of respective spectral features. We presume the composite spectrum to contain all individual bands present in both SWNTs and GO spectra, and the results obtained for those (number of spectral functions and their initial parameters) were used in order to perform fitting. The numerical data obtained is put into the Table 3 which summarizes the Raman bands parameters of all films analyzed in present study (see below). We have observed the spectral changes of Raman bands attributed to SWNTs and GO which indicate the noncovalent interaction between nanotubes and GO flakes in composite. First we provide the comparison between position of maximum and FWHM parameters of nanotube-related bands in SWNTs and GO-SWNTs spectra. We outline the 1–2 cm^{-1} frequency upshifts of G^- bands and more intense G^+ band (from 1592 cm^{-1} to 1593.1 cm^{-1}). The shifts of nanotube tangential bands can be caused by charge transfer between GO and SWNTs as well as mechanical stress and subsequent deformation [23]. As it follows from our results, the shift value is smaller than ~ 4.3 cm^{-1} upshift observed for composite film containing GO with metallic and semiconducting nanotubes (in ratio about 1:1 [23]). This indicates that the interaction between semiconducting carbon nanotubes and GO in the composite film is weaker than in film with metallic and semiconducting nanotubes. The linewidth of Lorentzian components fitting the G^- and G^+ bands also becomes approximately 1.5 times larger in the spectrum of GO-SWNTs composite film as compared to SWNTs one (except the weakest G^- Lorentzian located at 1520 cm^{-1}). Larger linewidth can be a consequence of more inhomogenuous nanotube environment in case of SWNT-GO and SWNT-SWNT interaction in composite, while only latter one is present in SWNTs film. The nanotube D band is upshifted by ~ 5 cm^{-1} in GO-SWNTs spectrum and becomes narrower (from 50 to 33 cm^{-1}). The changes of D band are often related to altered electronic structure of nanotubes, because it in turn defines the suitable non-zero wavevectors of phonons taking part in one-phonon one-elastic scattering process. The parameters of GO bands, especially of the G band, are changed at the composite formation as well. The FWHM value of the G band is increased from 111 cm^{-1} (GO film) to 138 cm^{-1} (GO-SWNTs film) while D band is practically unchanged. At that the frequencies of maximum of both G and D graphene oxide bands are changed by ~ 1 cm^{-1}, a near-negligible value given the large linewidth, however, this value matches with shifts of nanotube tangential bands. The GO bands integral intensity ratios D/G, D/D' and D'/G discussed in previous section when calculated for the composite film are 2.1, ~ 13 and 0.16. As these values are practically the same for GO film, the noncovalent interaction between nanotubes and graphene oxide in the composite does not noticeably alter defect-related properties of GO.

3.3. Raman spectroscopy of GO-SWNTs-GOx composite film: analysis and comparison with composite GO-SWNTs film

As the nanotubes and graphene oxide form porous, water-permeable conductive composite [12, 14] and free space is left between GO flakes and SWNTs, such structures can serve as a 3D container for molecules applicable for biosensing, i.e., enzymes. In our present study we have used the enzyme glucose oxidase (GOx) and have obtained GO-SWNTs-GOx composite similarly to method used for GO-SWNTs film. The Raman spectrum of the GO-SWNTs-GOx composite in the range of defect-induced and tangential modes is presented and compared with GO-SWNTs one in Figs. 4(a) and 4(b).

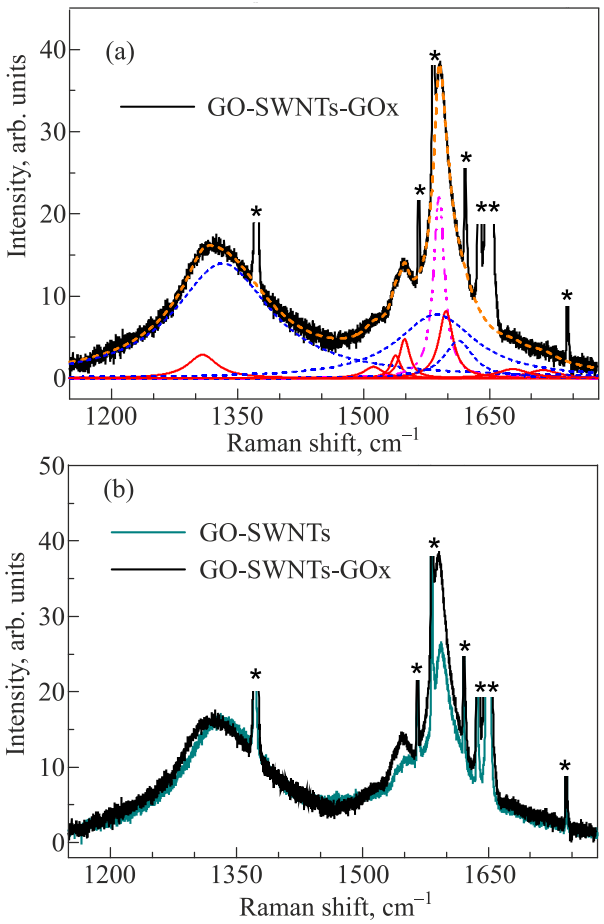

Fig. 4. (Color online) (a) Raman spectrum of the composite film that contains enzyme (GO-SWNTs-GOx). Deconvolution into individual spectral functions is shown, dashed (blue) and solid (red) lines under the experimental spectrum represent bands originating from GO and SWNTs respectively; the dash-dotted line (crimson,) is used for the band present in both SWNTs and GO films spectra (with maximum at 1593.1 cm^{-1}). Dashed line matching with the experimental spectrum represents the sum of all spectral functions. Asterisks * denote the He–Ne plasma lines. (b) Raman spectra of GO-SWNTs and GO-SWNTs-GOx composites normalized to equal integral intensity of wide GO tangential mode [peaked at 1586.5 cm^{-1} in Fig. 4(a)].

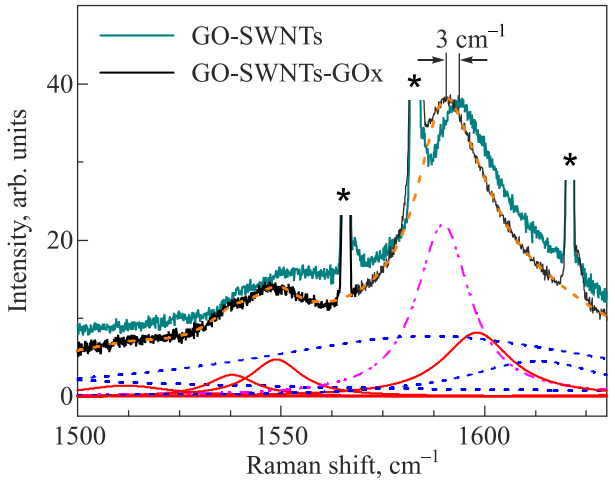

Fig. 5. (Color online) Raman spectra of GO-SWNTs and GO-SWNTs-GOx composites normalized to peak intensity of nanotube tangential band, frequency shift is denoted. Deconvolution into individual spectral functions is shown for GO-SWNTs-GOx, asterisks * denote the He–Ne plasma lines.

The mass ratio of GO and SWNTs at the preparation of composites was the same (1:1). Therefore it is possible to compare the relative intensities of GO and SWNTs Raman bands in both spectra. We have deduced that the integral intensity of nanotube-related bands is larger in the case of the GO-SWNTs-GOx composite as compared to GO-SWNTs one (see Fig. 4(b) and Table 3). Another prominent distinction between two spectra is the peak position of G^- and G^+ bands. These bands are noticeably downshifted in the GO-SWNTs-GOx spectrum as compared to GO-SWNTs one as is shown in detail in Fig. 5.

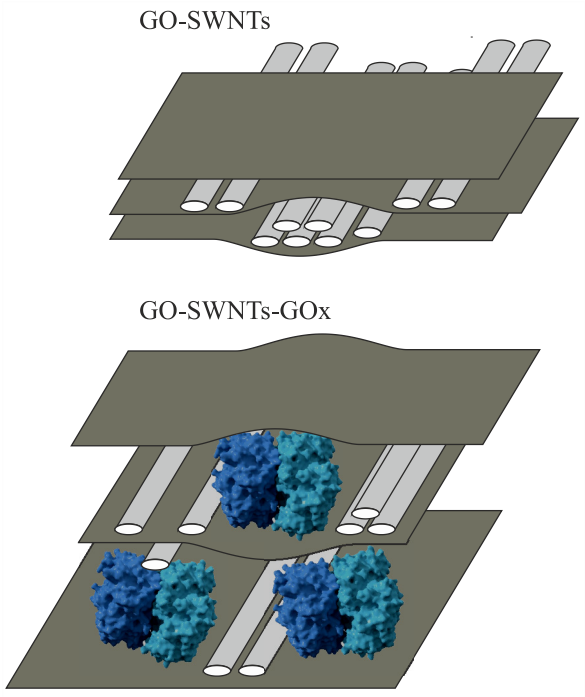

Fig. 6. (Color online) Schematic for GO-SWNTs composite films with (b) and without (a) enzyme glucose oxidase.

The shift of G^+ Lorentzians is 2–3 cm^{-1} and reaches 8 cm^{-1} in the case of G^-. At the same time, spectral position and FWHM of SWNTs bands become closer to the values obtained for single-component SWNTs film spectrum. Situation is qualitatively similar for G mode of GO, the parameters are almost the same if we compare GO and GO-SWNTs-GOx spectra. The "reverse" shift of nanotube G^+ and G^- bands for composite containing enzyme and overall more intense nanotube Raman spectrum can be caused by diminished mechanical stress as the SWNTs and GO flakes adjacent in GO-SWNTs composite tend to be separated by introduced GOx globules (~ 4 nm diameter), as is schematically shown in Fig. 6. In our opinion, these observations imply that the presence of GOx makes composite less dense and decreases the direct interaction between SWNTs and GO in the composite.

Conclusion

A noncovalent interaction between predominantly semiconducting carbon nanotubes and GO in composite films was analyzed using Raman spectroscopy in the range of D and G modes. Comparison of Raman spectra of composite films with spectra of components showed that charge transfer occurs between them as well as deformation of the carbon surface. The interaction is accompanied with band broadening and spectral shifting. So, this interaction caused the upshift of high-frequency tangential mode of nanotubes (G^+) by about 1–2 cm^{-1} in the composite film compared to SWNTs one. This value is smaller than shift observed for the composite film containing GO with metallic and semiconducting nanotubes in a ratio of about 1:1 (~ 4.3 cm^{-1}). This indicates that the interaction between semiconducting carbon nanotubes and GO in composite film is weaker than in film with metallic and semiconducting nanotubes.

An introducing of biological globules (enzyme glucose oxidase) in this composite film allows to weaken a mechanical stress of GO on the nanotubes. As a result, nanotube G^+ and G^- bands in the GO-SWNTs-GOx film spectrum are downshifted as compared to GO-SWNTs one.

The new information obtained in this work contributes to better understanding the physical mechanisms of the interaction among components of hybrid 3D nanostructures formed by low-dimensional carbon nanostructures including also biological macromolecules. The fabricated 3D nanostructures formed by nanotubes and graphene oxide are very useful for many potential applications such as production of supercapacitors and lithium batteries, layering conductive and transparent coverage, production of filters for water purification, development of different sensors including biosensors and so on.

Acknowledgements

This work has been supported by funding from the National Academy of Sciences of Ukraine under Grant 0120U100157. The authors are grateful to A. M. Plokhotnichenko for the samples preparation.

1. C. Cheng, S. Li, A. Thomas, N. A. Kotov, and R. Haag, *Chem. Rev.* **117**, 1826 (2017).
2. X.-M. Huang, L.-Z. Liu, S. Zhou, and J.-J. Zhao, *Front. Phys.* **15,** 33301 (2020).
3. W. Yu, L. Sisi, Y. Haiyana, and L. Jie, *RSC Adv.* **10**, 15328 (2020).
4. A. M. Dimiev and Siegfried Eigler, *Graphene Oxide*: *Fundamentals and Applications*, John Wiley & Sons Ltd., New York (2017).
5. M. V. Karachevtsev, S. G. Stepanian, A.Yu. Ivanov, V. S. Leontiev, V. A. Valeev, O. S. Lytvyn, L. Adamowicz, and V. A. Karachevtsev, *J. Phys. Chem. C* **121**, 18221 (2017).
6. S. Nardecchia, D. Carriazo, M. L. Ferrer, M. C. Gutierrrez, and F. del Monte, *Chem. Soc. Rev.* **42**, 794 (2013).
7. W. Fan, L. Zhang, and T. Liu, *Graphene-Carbon Nanotube Hybrids for Energy and Environmental Applications*, Springer, Singapore (2017).
8. A. B. Kaiser and V. Skakalova, *Chem. Soc. Rev.* **40**, 3786 (2011).
9. A. L. Hu, D. S. Hecht, and G. Gruner, *Chem. Rev.* **110**, 5790 (2010).
10. J. Zaumseil, *Semicond. Sci. Technol.* **30**, 074001 (2015).
11. V. Skakalova, A. B. Kaiser, Y.-S. Woo, and S. Roth, *Phys. Rev. B* **74**, 085403 (2006).
12. V. A. Karachevtsev and N. V. Kurnosov, *Fiz. Nizk. Temp.* **45**, 1300 (2019) [*Low Temp. Phys*. **45**, 1109 (2019)].
13. N. Kurnosov and V. Karachevtsev, *Temperature Dependence of Conductivity in Composite Film of Single-Walled Carbon Nanotubes with Graphene Oxide, in: Microstructure and Properties of Micro- and Nanoscale Materials, Films, and Coatings* (*NAP 2019*), A. Pogrebnjak and O. Bondar (eds.), Springer Proceedings in Physics, Springer, Singapore (2020), Vol. 240.
14. V. A. Karachevtsev, A. M. Plokhotnichenko, M. V. Karachevtsev, A. S. Linnik, and N. V. Kurnosov, *Fiz. Nizk. Temp.* **45**, 881 (2019) [*Low Temp. Phys.* **45**, 754 (2019)].
15. R. Saito, M. Hofmann, G. Dresselhaus, A. Jorio, and M. S. Dresselhaus, *Adv. Phys.* **60**, 413 (2011).
16. J.-B. Wu, M.-L. Lin, X. Cong, H.-N. Liu, and P.-H. Tan, *Chem. Soc. Rev.* **47**, 1822 (2018).
17. M. S. Dresselhaus, G. Dresselhaus, R. Saito, and A. Jorio, *Phys. Rep.* **409**, 47 (2005).
18. L. G. Cancado, A. Jorio, E. H. Martins Ferreira, F. Stavale, C. A. Achete, R. B. Capaz, M. V. O. Moutinho, A. Lombardo, T. S. Kulmala, and A. C. Ferrari, *Nano Lett.* **11**, 3190 (2011).
19. P. V. Kumar, N. M. Bardhan, G.-Y. Chen, Z. Li, A. M. Belcher, and J. C. Grossman, *Carbon* **100**, 90 (2016).
20. A Eckmann, A, Felten, A. Mishchenko, L. Britnell, R. Krupke, K. S. Novoselov, and C. Casiraghi, *Nano Lett.* **12**, 3925 (2012).
21. D. López-Díaz, M. López Holgado, J. L. García-Fierro, and M. M. Velázquez, *J. Phys. Chem. C* **121**, 20489 (2017).
22. K. Tsirka, A. Katsiki, N. Chalmpes, D. Gournis, and A. S. Paipetis, *Front. Mater.* **5**, 37 (2018).
23. A. Yu. Glamazda, S. G. Stepanian, M. V. Karachevtsev, A. M. Plokhotnichenko, L. Adamowicz, and V. A. Karachevtsev, *Physica E* **124**, 114279 (2020).
24. W. S. Hummers Jr. and R. E. Offeman, *J. Am. Chem. Soc.* **80**, 1339 (1958).
25. A. Jorio, A. G. Souza Filho, G. Dresselhaus, M. S. Dresselhaus, A. K. Swan, M. S. Unlu, B. B. Goldberg, M. A. Pimenta, J. H. Hafner, C. M. Lieber, and R. Saito, *Phys. Rev. B* **65**, 155412 (2002).
26. H. Telg, J. G. Duque, M. Staiger, X. Tu, F. Hennrich, M. M. Kappes, M. Zheng, J. Maultzsch, C. Thomsen, and S. K. Doorn, *ACS Nano* **6**, 904 (2012).
27. V. A. Karachevtsev, A. Yu. Glamazda, U. Dettlaff-Weglikowska, V. S. Leontiev, P. V. Mateichenko, S. Roth, and A. M. Rao, *Carbon* **44**, 1292 (2006).
28. V. A. Karachevtsev, A.Yu. Glamazda, E. S. Zarudnev, M. V. Karachevtsev, V. S. Leontiev, A. S. Linnik, O. S. Lytvyn, A. M. Plokhotnichenko, and S. G. Stepanian, *Ukr. J. Phys.* **57**, 700 (2012).
29. A. Kaniyoor and S. Ramaprabhu, *AIP Adv.* **2**, 032183 (2012).

Композитні плівки оксиду графену з напівпровідниковими вуглецевими нанотрубками: характеризація за допомогою раманівської спектроскопії

N. V. Kurnosov, V. A. Karachevtsev

Проаналізовано нековалентну взаємодію між напівпровідниковими одностінними вуглецевими нанотрубками (SWNTs) та оксидом графену (GO) у композитній плівці (GO-SWNTs) за допомогою раманівської спектроскопії у діапазоні *D*- та *G*-мод (1170–1780 см$^{-1}$). Порівняння раманівського спектру композитної плівки зі спектрами однокомпонентних плівок GO та SWNTs показало, що взаємодія між нанотрубками та оксидом графену супроводжується зсувом та збільшенням ширини смуг. Спектральні трансформації пов'язуються з перенесенням заряду, а також деформацією вуглецевих поверхонь в композиті. Спектральні дослідження композитної плівки GO-SWNTs з біологічними глобулярними молекулами (фермент глюкозооксидаза) показали, що ці молекули зменшують механічне напруження між оксидом графену та нанотрубками.

Ключові слова: оксид графену, одностінні вуглецеві нанотрубки, композитні плівки, нековалентна взаємодія, раманівська спектроскопія.